# A novel mechanism of gene regulation and tumor suppression by the transcription factor FKHR

Shivapriya Ramaswamy,[1,4] Noriaki Nakamura,[1,4] Isabelle Sansal,[1] Louise Bergeron,[2] and William R. Sellers[1,3]

[1]Department of Adult Oncology and Department of Internal Medicine, Dana-Farber Cancer Institute and Brigham and Women's Hospital, Harvard Medical School, Boston, Massachusetts 02115
[2]Division of Oncology, Millennium Pharmaceuticals, Cambridge, Massachusetts 02139
[3]Correspondence: william_sellers@dfci.harvard.edu
[4]These authors contributed equally to this work.

**Summary**

**The mammalian DAF-16-like transcription factors, FKHR, FKHRL1, and AFX, function as key regulators of insulin signaling, cell cycle progression, and apoptosis downstream of phosphoinositide 3-kinase. Gene activation through binding to insulin response sequences (IRS) has been thought to be essential for mediating these functions. However, using transcriptional profiling, chromatin immunoprecipitation, and functional experiments, we demonstrate that rather than activation of IRS regulated genes (Class I transcripts), transcriptional repression of D-type cyclins (in Class III) is required for FKHR mediated inhibition of cell cycle progression and transformation. These data suggest that a novel mechanism of FKHR-mediated gene regulation is linked to its activity as a suppressor of tumor growth.**

## Introduction

Inappropriate activation of phosphoinositide 3-kinase (PI3K) signaling is intimately connected with the acquisition of a transformed phenotype. Certain retroviruses and DNA tumor viruses transform rodent and avian cells through activation of this pathway. Similarly, in human tumors, genetic alterations of this pathway, including amplification of *PI3KCA, AKT1,* and *AKT2* genes and mutation of the *PTEN* tumor suppressor, lead to constitutive activation of Akt family members and constitutive phosphorylation of Akt substrates (reviewed in Vazquez and Sellers, 2000).

The *PTEN* tumor suppressor gene encodes a lipid phosphatase that specifically dephosphorylates the D3 position of phosphatidylinositol 3,4,5-trisphosphophate and phosphatidylinositol 3,4-bisphosphate (Maehama and Dixon, 1999). In this capacity, PTEN antagonizes PI3K signaling and regulates the subsequent activation of Akt (reviewed in Vazquez and Sellers, 2000). In cells lacking PTEN, substrates of Akt are aberrantly phosphorylated.

In *C. elegans,* the genetic evidence points to a convergence of the PI3K/Akt signaling pathway, and in particular of Akt action, upon the DAF-16 winged-helix transcription factor (Lin et al., 1997; Ogg et al., 1997). The mammalian homologs of DAF-16, AFX, FKHRL1, and FKHR (hereafter referred to as forkhead) are each substrates for Akt kinase activity (Brunet et al., 1999; del Peso et al., 1999; Kops et al., 1999; Rena et al., 1999; Takaishi et al., 1999; Tang et al., 1999). Akt phosphorylation of these forkhead transcription factors induces binding to 14-3-3 proteins, relocalization to the cytoplasm, and impairment of transcriptional activity (Biggs et al., 1999; Brunet et al., 1999; Takaishi et al., 1999; Tang et al., 1999; Tomizawa et al., 2000).

In PTEN null cells, these factors are constitutively phosphorylated and hence constitutively cytoplasmic. Thus, when exogenously expressed, they are incapable of activating FKHR responsive promoters (Nakamura et al., 2000). A phosphosite mutant form of FKHR (FKHR;AAA), in which the three Akt phosphorylation sites are altered (S→A), is immune to Akt regulation. In PTEN null cells, this mutant is constitutively nuclear and strongly activates FKHR responsive promoters. FKHR;AAA thus restores FKHR transcriptional activity to PTEN null cells. We previously found that reconstitution of forkhead activity was sufficient to restore the induction of apoptosis in PTEN null cells that likewise undergo apoptosis upon PTEN reconstitution. These data are in keeping with other published data demonstrating a role for these forkhead factors in regulating apoptosis (Brunet et al., 1999; Tang et al., 1999). Moreover, reconstitution of FKHR activity did not induce apoptosis, but rather was sufficient for the induction of a G1 cell cycle arrest in those PTEN

### SIGNIFICANCE

**Emerging data suggest that FKHR, AFX, and FKHRL1, each a substrate for the oncogenic Akt kinases, are critical downstream targets of the insulin/PI3K signaling pathway. In human tumors, this pathway is frequently deregulated, and these forkhead transcription factors are inactivated as a result of *PTEN* gene mutation. Thus, these forkhead factors are likely nonfunctional in a broad spectrum of human tumors. The data presented here suggest that a novel mechanism of transcriptional regulation, specifically repression of D-type cyclin transcription, rather than IRS dependent gene activation, accounts for the function of FKHR as a suppressor of tumor cell growth. These data begin to elucidate how, mechanistically, cell growth regulation differs from the other functional outputs downstream of FKHR.**

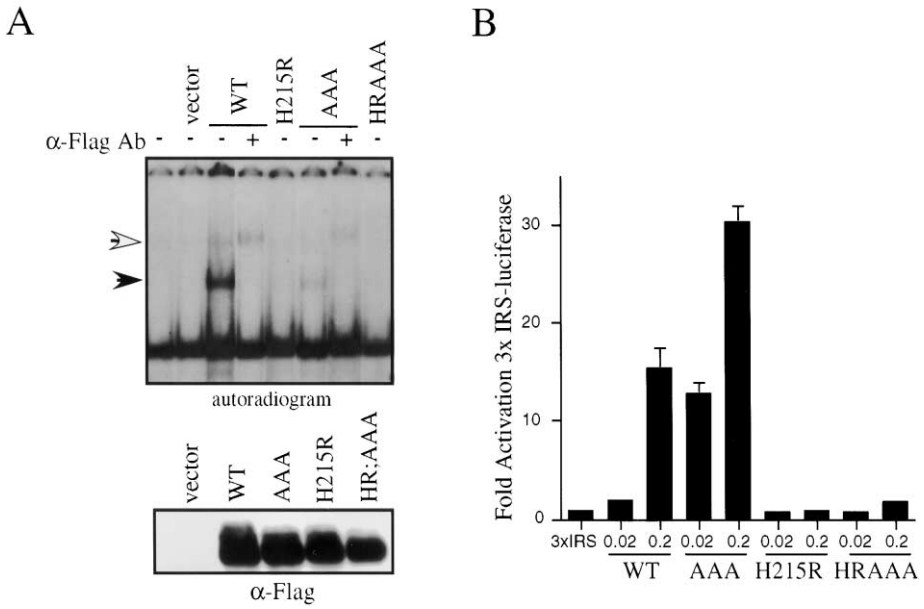


**Figure 1.** DNA binding and 3xIRS promoter activation by FKHR proteins

**A:** (Top panel) Mutation of FKHR residue H215 abolishes binding to an IRS. Extracts from U2-OS cells transfected with plasmids encoding the indicated FKHR proteins were incubated with a $^{32}P$ labeled double-stranded IRS oligonucleotide probe, in either the presence or absence of anti-Flag antibody. The solid arrow indicates the DNA-FKHR complex. The open arrow indicates the DNA-FKHR-antibody complex. (Bottom panel) Immunoblot detection of the indicated Flag-FKHR proteins.

**B:** Mutation of FKHR residue H215 abrogates transactivation of the 3xIRS promoter. U2-OS cells were transfected with the 3xIRS reporter plasmid and pCMV-β-Gal along with either 0.2 or 0.02 μg of the indicated FKHR expression plasmids. Cell lysates were prepared, and luciferase activity was measured and normalized to β-galactosidase activity. Results shown are representative of multiple independent experiments.

null cells that arrest in G1 upon PTEN reconstitution (Nakamura et al., 2000). Medema et al. likewise showed that these forkhead transcription factors can act as cell-cycle regulators and do so through transcriptional regulation of p27 (Medema et al., 2000). Together, these data suggest that forkhead factors are key mediators of tumor suppression downstream of PTEN.

In order to understand the mechanisms by which FKHR acts as a cell cycle regulator and tumor suppressor, as distinct from other functional outputs attributed to forkhead such as metabolic regulation or apoptosis, expression profiling was performed to identify transcriptional targets of FKHR that regulate cell proliferation and cellular transformation.

Three classes of FKHR regulated transcripts were identified. Class I genes were activated by FKHR, required IRS binding activity, and included the IRS regulated gene *IGFBP1*. Class II genes, including *Cbl-b*, *SOD-2*, and several DNA-damage response genes, comprise a major new class of genes (Class IIa) induced by FKHR without a strict requirement for interaction with an IRS element. Cell cycle regulation and suppression of transformation did not require direct DNA binding to IRS regulated promoters, nor the activation of the *IGFBP-1* gene cluster. Instead, transcriptional profiling and functional experiments demonstrated that cell cycle inhibition, soft agar growth suppression, and tumor suppression correlated with the transcriptional downregulation of a set of genes (Class III genes) that included *cyclin D1* and *D2*. Coexpression of cyclin D1 and Cdk4 bypassed the G1 arrest induced by FKHR;AAA, suggesting that such downregulation is necessary for the G1 arrest induced by FKHR. These data suggest that a novel mechanism of transcriptional regulation, specifically transcriptional inhibition or repression, accounts for FKHR tumor suppressor activity and is separable mechanistically from the induction of IRS regulated genes.

## Results

### Induction of FKHR activity in PTEN null cells

In order to understand how FKHR mediates tumor suppressor functions downstream of PTEN, we sought to identify the relevant FKHR transcriptional targets in PTEN null cells. To do so, cDNA array-based transcriptional profiling experiments were performed using adenoviral expression of FKHR;AAA to uniformly restore FKHR activity to PTEN null 786-O renal carcinoma cells.

Forkhead transcription factors, such as HNF3, bind to DNA as monomers primarily through helix 3 of the winged-helix domain (Clark et al., 1993; Jin et al., 1999). Sequence homology and the NMR structure of AFX suggest that FKHR, AFX, and FKHRL1 likely bind to an IRS element in a similar manner (Weigelt et al., 2001). Mutation of a conserved histidine to arginine in helix 3 abrogates DNA binding in members of this family, and introduction of the H215R mutation in FKHR (FKHR;H215R) or in FKHR;AAA (FKHR;HRAAA) abolished both binding to the *IGFBP-1* insulin response element (IRS) in gel shift assays (Figure 1A) and FKHR-mediated activation of a 3xIRS-luciferase reporter (Figure 1B) (Tang et al., 1999). FKHR;HRAAA was hence compared to FKHR;AAA in the profiling experiments.

A time course of activation of a 3xIRS promoter-luciferase reporter was used to estimate the likely temporal pattern of endogenous gene induction following adenoviral mediated expression of FKHR;AAA. To this end, 786-O cells were transfected with the 3xIRS promoter luciferase reporter plasmid and then infected with either Ad-Vector or Ad-FKHR;AAA. Luciferase activity was assayed from cells harvested at the indicated time points (Figure 2A). Ad-FKHR;AAA induced activation of the 3xIRS promoter at 12 hr, and this activity increased through the final time point of 24 hr to a maximum of 6-fold (Figure 2A). Therefore, a time course of 0 to 28 hr was chosen.

### Expression profiling

Three independent expression profiling experiments were carried out. In experiment 1, 786-O cells infected with Ad-Vector or Ad-FKHR;AAA were collected at 16, 20, 24, and 28 hr after infection. In experiment 2, 786-O cells infected with Ad-Vector or Ad-FKHR;AAA were collected at 0, 12, 16, 20, 24, and 28 hr. In experiment 3, 786-O cells infected with Ad-Vector, Ad-

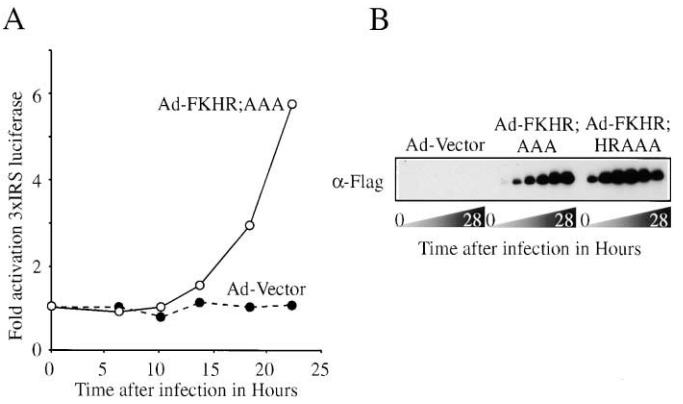


**Figure 2.** Promoter activation and protein production after infection with Ad-FKHR;AAA

**A:** Time course of promoter activation following infection with Ad-FKHR;AAA. 786-O cells were transfected with 3xIRS reporter plasmid and pCMV-β-gal and then infected (MOI of 30) with Ad-Vector (filled circles) or Ad-FKHR;AAA (open circles). Normalized luciferase activity was determined at the indicated time points following infection.

**B:** Time course of FKHR;AAA or FKHR;HRAAA protein production following adenovirus infection of 786-O cells (from experiment 3 of Figure 3). 786-O cells were infected with the indicated adenoviruses. Cell lysates prepared at 4 hr intervals after infection were immunoblotted with anti-Flag antibody.

FKHR;AAA, or FKHR;HRAAA were collected at 0, 8, 12, 16, 20, 24, and 28 hr. The production of the FKHR;AAA and FKHR;HRAAA proteins from experiment 3 is shown in Figure 2B. $^{32}$P-radiolabeled cDNA was generated by oligo-dT primed reverse transcription from total RNA. For each time point, equivalent amounts of radiolabeled cDNA were hybridized in replicate to nylon arrays containing either 30,000 cDNAs (30K array) (experiments 1 and 2) or 60,000 cDNAs (60K or whole genome array) (experiment 3). The normalized expression data files for experiments 1, 2, and 3 are available at http://research.dfci.harvard.edu/sellerslab/datasets/index.html.

After application of a minimal intensity (0.8 arbitrary units) and 1.5-fold variation filter, the expression data from experiment 3 was initially organized by K-means clustering into 60 groups (Herwig et al., 1999). cDNAs found in clusters in which the pattern of expression indicated adenoviral effect were eliminated, as were cDNAs in which gene expression variation over time was found in only one of the replicates (typically, these represented a variation in only a single time point in one replicate). The expression data from the remaining cDNAs were refiltered to exclude those not passing a 2-fold variation filter and were reorganized into 8 clusters. One cluster continued to represent expression patterns consistent with poor replicate data, and the remaining 7 clusters represented 4 dominant patterns of expression. Thus, after eliminating cDNAs with poor replicate data, the remaining cDNAs (665) were reorganized by K-means into 4 clusters (Figure 3A). 487 cDNAs from experiment 3 in these 4 clusters were also present on the arrays used in experiments 1 and 2 and are shown in Figure 3A. These cDNAs do not represent unique genes, but rather a combination of unique genes, ESTs, and, in some cases, more than one cDNA for the same gene. The temporal pattern of gene expression after infection with Ad-Vector, Ad-FKHR;AAA, and Ad-FKHR;HRAAA found in these 4 clusters is shown in Figure 3A.

In parallel, after eliminating duplicate cDNA probes, the 198 putative unique genes whose expression was altered in FKHR;AAA expressing cells by at least 2-fold (induced or repressed) at the 24 hr time point in both experiments 1 and 2 were selected. The data from experiments 1, 2, and 3 for this highly reproducible set were organized by hierarchical clustering (Eisen et al., 1998) of the log-transformed ratio data (the ratio of either FKHR;AAA or FKHR;HRAAA to the vector at each time point) (Figure 3B). Again, 4 major patterns of transcriptional regulation were seen and were similar to those found by K-means clustering. A number of genes apparently regulated in experiments 1 and 2 did not reproduce in experiment 3 (indicated by the brackets in Figure 3B). This may have resulted from a change in the performance characteristics of the cDNA probes on the 60K array or possibly from changes in annotation. Not surprisingly, FKHR (black arrow in Figure 3B) itself, presumably produced from the adenovirus, was the earliest induced gene.

Based upon these analyses, 4 classes of genes whose expression was altered in these experiments were defined (Figure 3 and Supplemental Tables S1–S4 at http://www.cancercell.org/cgi/content/full/2/1/81/DC1). Class I transcripts were those induced by FKHR;AAA, but not by the vector, nor by the FKHR;HRAAA mutant. Typified by *IGFBP-1*, members of this class included *DEPP*, lumican, decorin, ceruloplasmin, semaphorin E, and C-type lectin, as well as a number of ESTs. FKHR;AAA-specific induction was independently confirmed by real-time quantitative reverse transcriptase-polymerase chain reaction (Q-PCR) (for *DEPP*, semaphorin E, and *IGFBP-1*), by Northern analysis (*DEPP*), and by immunoblot detection (*IGFBP-1* and *DEPP*) (Figure 4A, Supplemental Figure S1, and data not shown).

The promoters of the *PEPCK* and *G6P* genes each contain IRS elements that, in reporter constructs, can be activated by forkhead (Ayala et al., 1999; Hall et al., 2000; Schmoll et al., 2000; Yeagley et al., 2001). Similarly, the *FasL* and *Bim-1* promoters contain FKHR response elements, are activated by FKHRL1, and are thought to mediate apoptosis in response to FKHRL1 activation (Brunet et al., 1999; Dijkers et al., 2000). cDNA probes for these and other genes whose promoters contain insulin response elements, including tyrosine aminotransferase and apolipoprotein C III, were present on the arrays, but were not induced by FKHR;AAA expression (Supplemental Figure S2). Thus, while adenoviral directed expression of FKHR strongly activated *IGFBP-1* and other Class I targets, such overexpression did not result in generalized transcriptional induction of putative IRS-containing promoters.

Class II was comprised of genes induced by FKHR;AAA, and to a varying extent or to a greater extent by FKHR;HRAAA (Class IIa and Class Iib, respectively). Class IIa genes included *Cbl-b*, *Dyrk-2*, Superoxide dismutase 2 (*SOD2*), and Damage-specific DNA binding protein 1 (*DDB1*). The expression pattern of Cyclin G2 and *BTG1*, while found in Class I by K-means clustering, fell into the same tree with *Cbl-b* when analyzed by hierarchical clustering. In independent experiments, immunoblotting showed that the protein for Cbl-b, a known regulator of PI3K signaling, was induced by both FKHR;AAA and FKHR;HRAAA, while Cyclin G2 expression was confirmed by Q-PCR (Figure 4B).

Class IIb genes were induced by FKHR;HRAAA to a greater extent than by FKHR;AAA. The most prominent known members of this class were *SLC5A3*, also known as $Na^+$ myo-inositol cotransporter, and *Mxi-I* (Figure 4C). Independent Q-PCR and

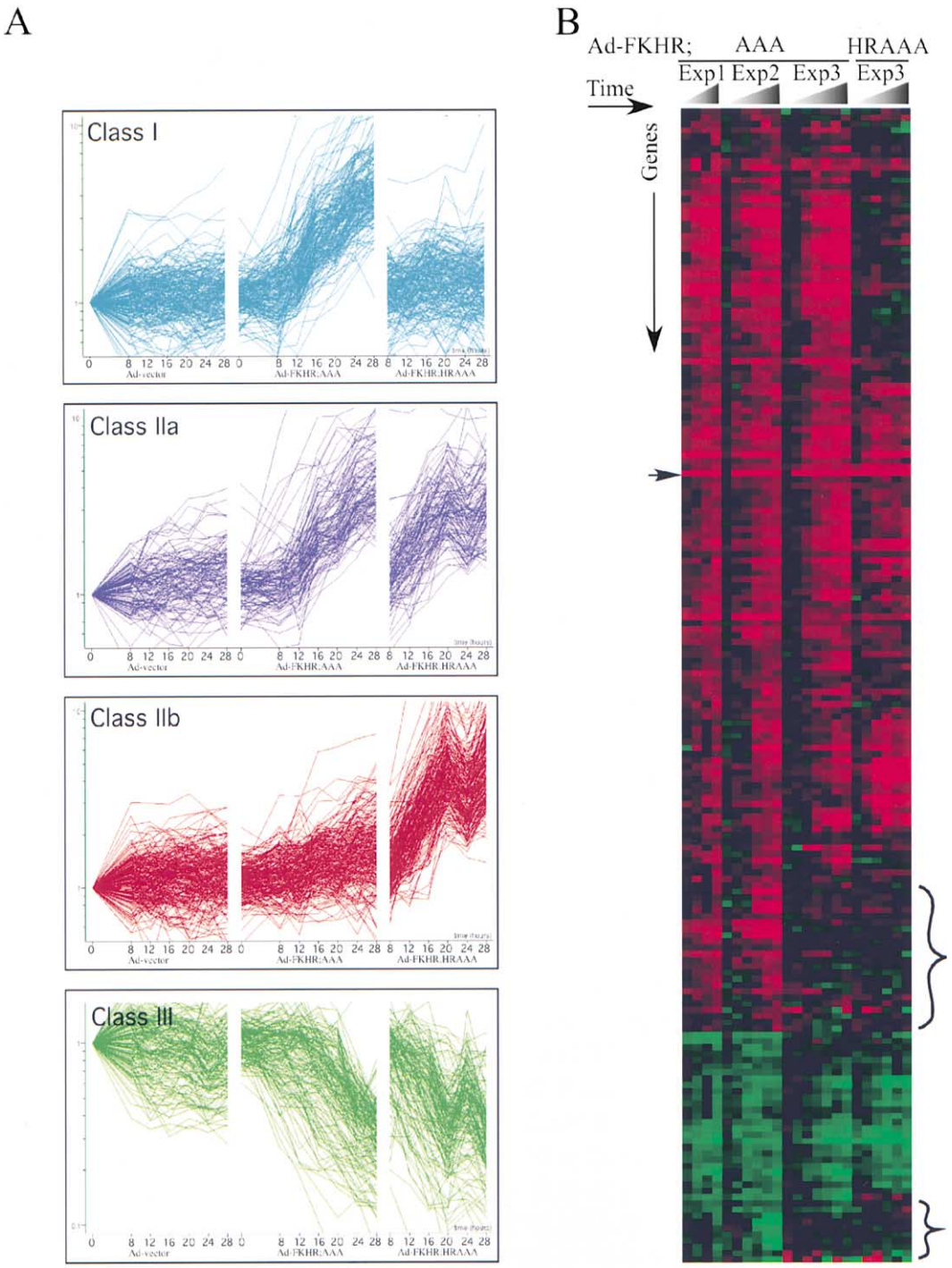


**Figure 3.** Genome-wide patterns of transcriptional regulation by FKHR

Three independent transcriptional profiling experiments were carried out in 786-O renal carcinoma cells as described in the methods.
**A:** The final 4 clusters as organized by K-means analysis as described in the text.
**B:** 198 genes that were at least 2-fold induced or repressed in the first two experiments were organized by hierarchical clustering using the data from all three experiments. The solid arrow indicates FKHR (which is detected on the arrays). Brackets indicate genes whose expression was induced or repressed in experiments 1 and 2, but not 3.

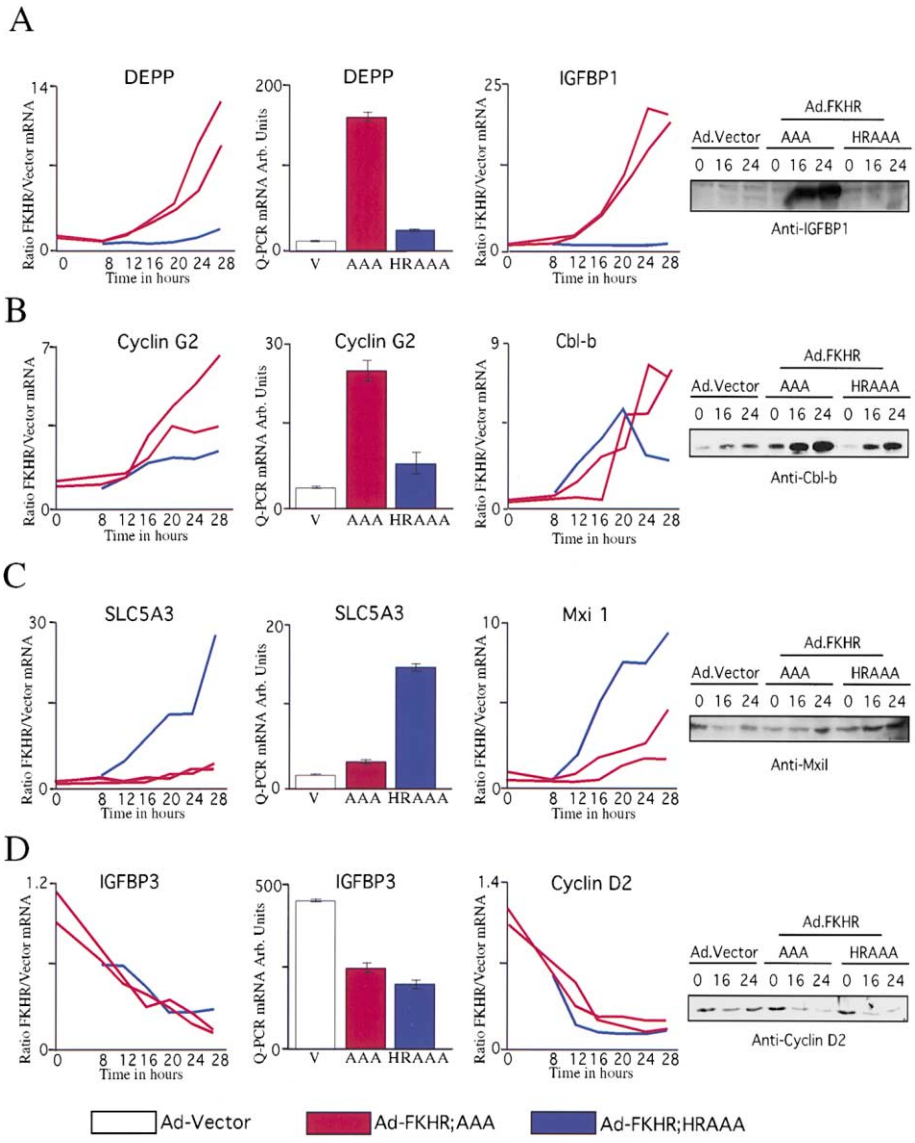


**Figure 4.** Validation of selected transcriptional targets

**A:** Class I targets DEPP and IGFBP-1.
**B:** Class IIa transcripts Cyclin G2 and Cbl-b.
**C:** Class IIb transcripts SLC5A3 and Mxi1.
**D:** Class III transcripts IGFBP3 and Cyclin D2. The indicated members of each class were validated either by measuring mRNA production at 24 hr after adenoviral infection of either Ad-vector (white), Ad-FKHR;AAA (red), or FKHR;HRAAA (blue) by quantitative real-time PCR (second panel of **A**, **B**, **C**, and **D**), or by immunoblotting (fourth panel of **A**, **B**, **C**, and **D**), and are shown compared to the temporal pattern of expression found in experiments 2 and 3 (first and third panels of **A**, **B**, **C**, and **D**). Red indicates infection with FKHR;AAA in experiments 2 or 3, and blue indicates infection with FKHR;HRAAA in experiment 3.

immunoblotting experiments confirmed that in both cases, induction was greater with the FKHR;HRAAA mutant (Figure 4C).

Class III genes, including Cyclin D2, Cyclin D1, epiregulin, and *IGFBP-3* (Figures 3A and 3B), were strongly downregulated by both FKHR;AAA and FKHR;HRAAA. Q-PCR for *IGFBP-3* and immunoblot detection of Cyclin D2 again confirmed the pattern of downregulation detected on the arrays (Figure 4D).

**FKHR;HRAAA is recruited to Class II and III promoters**

Class I transcripts, such as *IGFBP-1* and *DEPP*, were induced by FKHR;AAA, but not FKHR;HRAAA. If these are direct targets of FKHR transcription, a prediction is that FKHR;AAA, but not FKHR;HRAAA, should be found bound in vivo to the promoters of these genes. To test this prediction, in vivo crosslinked chromatin was prepared from cells expressing Ad-Vector, Ad-FKHR;AAA, or Ad-FKHR;HRAAA and immunoprecipitated with anti-flag antibody. The bound DNA was extracted and amplified using primers to the *IGFBP-1* and *DEPP* promoters. Indeed, FKHR;AAA, but not FKHR;HRAAA, was found in complex with the *IGFBP-1* and *DEPP* promoters (Figure 5). These data suggest that these genes are likely directly activated by FKHR binding to IRS or IRS-like promoter elements.

On the other hand, class II and III transcripts were regulated both by wild-type FKHR;AAA and, at least in part, by a FKHR protein (FKHR;HRAAA) that does not interact with IRS elements in vitro (Figure 1) or with Class I promoters in vivo (Figure 5). Nonetheless, FKHR;HRAAA might retain the ability to interact with promoter elements either through a second transcription factor or through an alternate DNA recognition element. To test this hypothesis, the DNA extracted from immunoprecipitated chromatin was also amplified with primers for the Cyclin G2 and Cyclin D1 promoters. Here, the Cyclin G2 (Class II) and Cyclin D1 (Class III) promoters were found in association with both FKHR;AAA and FKHR;HRAAA. Thus, FKHR;HRAAA retained the ability to bind these promoters (Figure 5). These data are consistent with the notion that FKHR can interact with promoters through direct or indirect binding to an as yet undefined promoter element(s) (hereafter referred to as IRS-indepen-

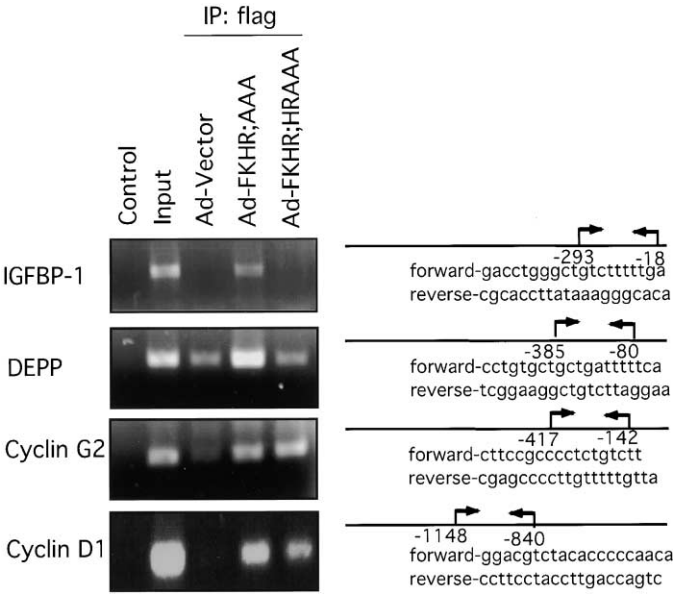


**Figure 5.** Chromatin immunoprecipitation of FKHR-promoter complexes

In vivo crosslinked chromatin was prepared from 786-O cells infected with the indicated adenoviruses and immunoprecipitated with anti-Flag antibody. Bound promoters were detected by PCR amplification using the indicated primer pairs specific for the IGFBP-1, DEPP, Cyclin G2, and Cyclin D1 promoters (as indicated). Control lanes represent no DNA, while input represents DNA extracted from chromatin prior to immunoprecipitation.

dent binding). In keeping with these data, transcriptional regulation by FKHR through binding to nuclear receptors has been observed by two groups (Schuur et al., 2001; Zhao et al., 2001), as well as in our lab (I.S. and W.R.S., unpublished data).

### FKHR;HRAAA retains the ability to inhibit cell cycle progression and suppress tumor formation

The transcriptional profiling data raised the possibility that FKHR-mediated G1 cell cycle regulation might be separable from FKHR activation of IRS-dependent genes such as *IGFBP-1* (and other Class I transcripts). To test this hypothesis, the cell cycle distribution of PTEN null 786-O cells infected with either backbone retrovirus or retroviruses directing the expression of the indicated FKHR proteins was determined (Figure 6A). In keeping with published data, neither FKHR;WT nor FKHR;H215R expression (both cytoplasmic in these cells) led to an accumulation of cells in G1. However, both FKHR;AAA- and FKHR;HRAAA-expressing cells accumulated in G1. 786-O cells infected with the same retroviruses were also tested for their ability to grow in semisolid media. Here, both FKHR;AAA and FKHR;HRAAA, but not the vector or FKHR;WT, suppressed the outgrowth of soft agar colonies (Figure 6C).

Finally, $1 \times 10^5$ stably transduced 786-O cells were injected into the flanks of nude mice. In each example, the right flank was injected with vector-transduced cells, while the left flank of the same mouse was injected with cells expressing either FKHR;AAA or FKHR;HRAAA. In this experiment, 6 sites injected with vector containing cells formed large, rapidly progressive tumors. In these same animals, a small tumor formed at 1 of the 2 sites injected with FKHR;AAA, while no tumors were seen at 4 sites injected with FKHR;HRAAA (Figure 6D).

### FKHR;AAA and FKHR;HRAAA induce growth arrest in U87-MG cells

In order to ask whether the results obtained in 786-O cells could be extended to other PTEN null cells, PTEN null U87-MG glioblastoma cells were used. These cells undergo a G1 arrest and growth retardation upon restoration of PTEN or upon restoration of the FKHR-related proteins FKHRL1 and AFX (Cheney et al., 1998; Furnari et al., 1997, 1998; Medema et al., 2000). We therefore asked whether FKHR;AAA or the DNA binding mutant were able to suppress the growth of these cells. To this end, stable polyclonal pools of U87-MG cells containing the vector or expressing FKHR;WT, FKHR;AAA, FKHR;H215R, and FKHR;HRAAA were generated by retroviral transduction followed by puromycin selection. The growth rates of such cells were significantly retarded by both FKHR;AAA and FKHR;HRAAA (Figure 7A). Interestingly, numerous U87-MG cells infected with FKHR;AAA and FKHR;HRAAA developed a "flat cell" morphology reminiscent of cells undergoing cellular senescence. These cells were also found to have detectable, senescence-associated β-galactosidase (SA-β-gal) activity. SA-β-gal positive "flat" cells were abundantly present in cultures of cells stably expressing either FKHR;AAA or FKHR;HRAAA, but not in cells infected with the backbone retrovirus or with FKHR;H215R or FKHR;WT (Figure 7B and data not shown). Thus, the growth inhibitory properties of FKHR;AAA and FKHR;HRAAA can be extended to a second PTEN null cell line.

### FKHR;HRAAA is unable to induce cell death

PTEN null LNCaP prostate adenocarcinoma cells undergo cell death following reconstitution with either PTEN or FKHR;AAA. FKHRL1, another member of the Akt-regulated forkhead transcription factor subfamily, induces apoptosis in Rat1 cells and can regulate the promoter of the death effector ligand FasL or Bim1 (Brunet et al., 1999; Dijkers et al., 2000). In order to ask whether, in addition to suppressing proliferation, FKHR;HRAAA also retained apoptotic functions, LNCaP cells were infected with amphotropic backbone retrovirus or retrovirus encoding FKHR;WT, FKHR;AAA, FKHR;H215R, and FKHR;HRAAA. After puromycin selection, cell viability was determined. While FKHR;AAA completely suppressed cell viability, infection with the retrovirus encoding FKHR;HRAAA did not induce cell death, while viable expressing cells comparable in number to the control infections were obtained (Figure 6B).

Taken together, these data suggest that the mechanism of FKHR-mediated cell cycle regulation and tumor suppression is completely distinct from both the activation of typical FKHR target genes, such as *IGFBP-1*, and from the mechanisms underlying FKHR mediated apoptosis. The latter functions appear to require binding to an IRS element and induction of IRS dependent gene transcription, while the former do not.

### D-type Cyclin proteins are downregulated in cells expressing FKHR;AAA or FKHR;HRAAA

Our data strongly suggest that a novel IRS-independent mechanism of gene regulation accounts for FKHR growth suppression function. Furthermore, the results of the transcriptional profiling experiments suggested that both FKHR;AAA and FKHR;HRAAA could repress certain transcripts—in particular, D-type cyclins. To confirm downregulation of cyclin D1 and D2, protein extracts were prepared from U87-MG cells at 0, 24, 36, and 48 hr after infection with Ad-Vector, Ad-FKHR;AAA, or Ad-FKHR;HRAAA.

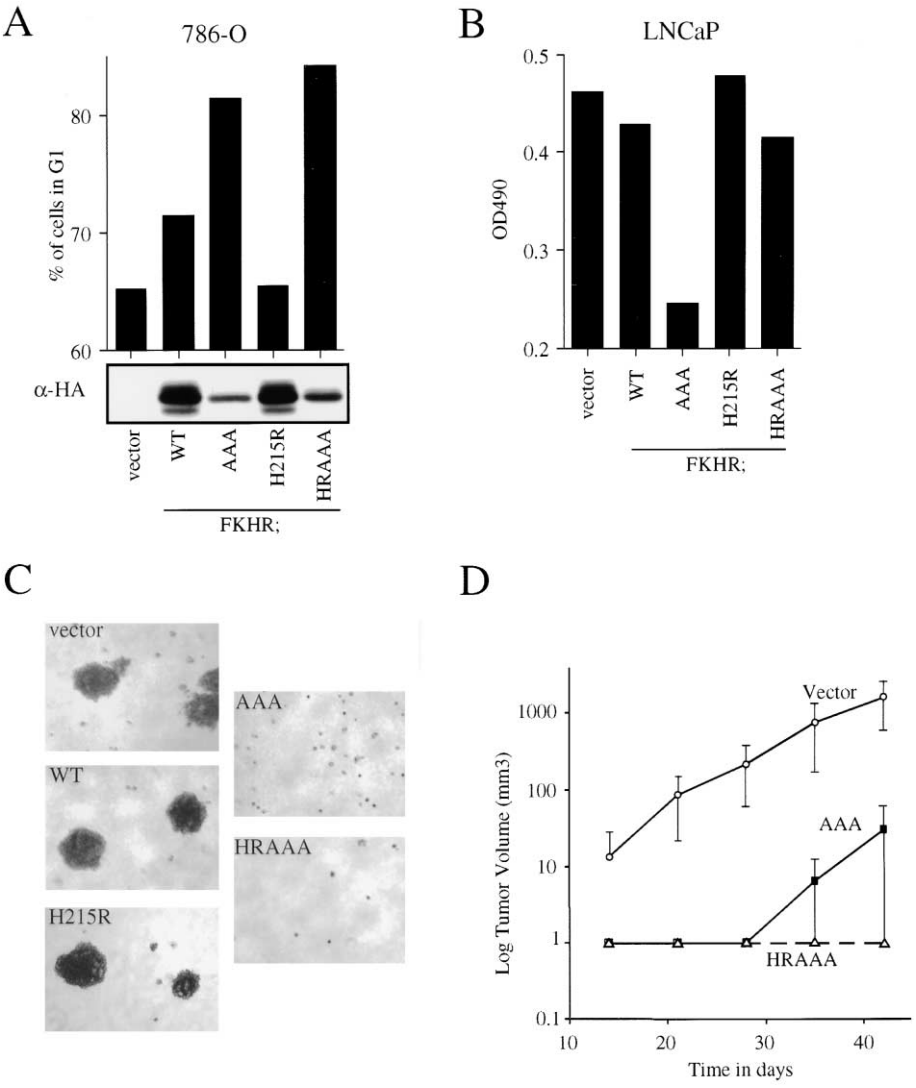


**Figure 6.** FKHR;HRAAA retains FKHR growth and tumor suppressor activities but fails to induce cell death

**A:** FKHR;HRAAA induces a G1 arrest. The cell cycle distribution of 786-O cells infected with backbone retrovirus or retroviruses encoding the indicated FKHR proteins was analyzed by FACS analysis of PI stained cells harvested 48 hr after infection. The level of expression of the different FKHR was detected by anti-HA immunoblot, and the results are shown in the bottom panel.

**B:** FKHR;HRAAA fails to induce apoptosis in LNCaP cells. LNCaP cells were infected with the retrovirus as in **A**. Cell viability was measured by MTS assay after selection for 4 days in puromycin.

**C:** FKHR;HRAAA suppresses colony formation in soft agar. 786-O cells stably expressing the indicated FKHR protein, generated by retroviral infection, were mixed with DMEM containing 0.3% agarose and plated onto DMEM containing 0.6% agarose. Soft agar colonies were photographed after 4 weeks. The results obtained are representative of three independent experiments.

**D:** FKHR;HRAAA inhibits xenograft tumor formation in nude mice. $1 \times 10^5$ second passage 786-O cells infected with the indicated retroviruses were injected into the flanks of nude mice. The tridimensional tumor measurements were made weekly and used to calculate tumor volume. In order to show the growth obtained in one FKHR;AAA-expressing line, the results are presented as log-tumor volume. The mean and standard error of each tumor or injection site is shown. For the purposes of plotting on a log-scale, injections sites where no tumor growth was seen were arbitrarily set to 1 $mm^3$.

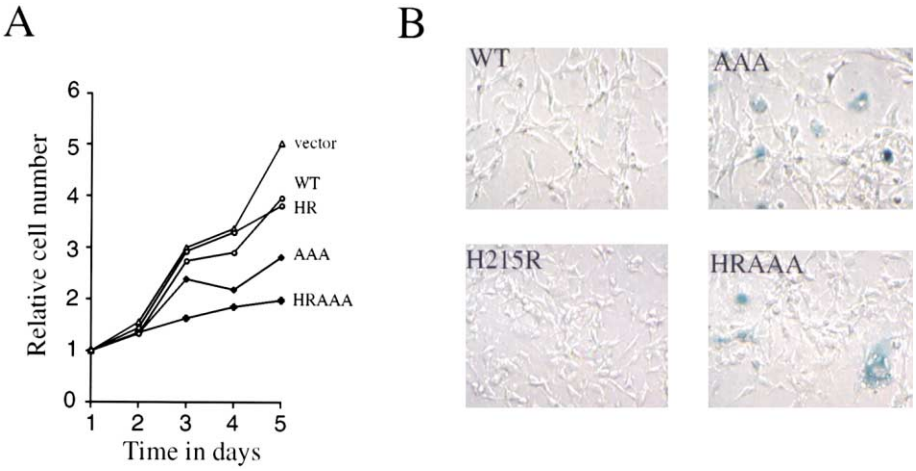


**Figure 7.** FKHR;AAA and FKHR;HRAAA inhibits cell growth and induces a senescence phenotype in U87MG cells

**A:** U87-MG cells were infected with retroviral supernatant directing the expression of the indicated FKHR proteins. Stable polyclonal cell populations were isolated by puromycin selection, and the number of viable cells at the indicated days after infection was determined using MTS assay as described in the Experimental Procedures.

**B:** U87-MG cells expressing the indicated FKHR proteins were generated by retroviral infection as in A. Five days after selection in puromycin, the cells were stained for SA-β-gal activity to determine the senescence phenotype as described in the Experimental Procedures. These results were representative of three independent experiments.

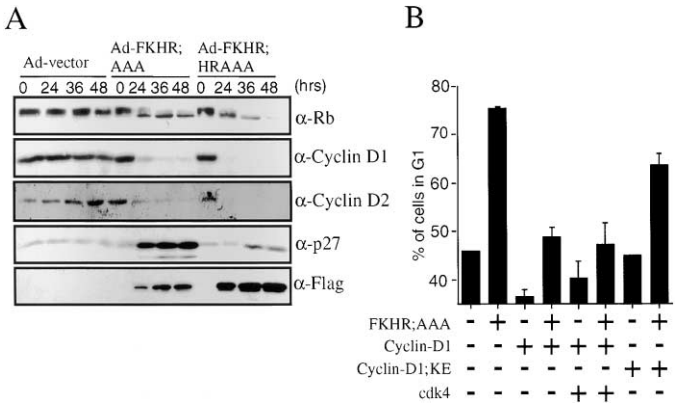


**Figure 8.** Downregulation of D-type cyclins by FKHR;AAA and FKHR;HRAAA is required for induction of a cell cycle arrest

**A:** U87-MG cells were infected with Ad-Vector, Ad-FKHR;AAA, and Ad-FKHR;HRAAA. Protein lysates were prepared at the indicated time points after infection and immunoblotted with anti-Rb, anti-cyclin D1, anti-cyclin D2, anti-p27, and anti-FLAG antibodies.

**B:** Coexpression of Cyclin D1 overrides a FKHR;AAA mediated G1 arrest. 786-O cells were transfected with a plasmid encoding for CD19 and either vector or a plasmid encoding FKHR;AAA ,either alone or together with plasmids directing the expression of Cyclin D1;WT, Cyclin D1;WT, and Cdk4, and Cyclin D1;KE. The transfected cells were fixed, and stained with FITC-conjugated anti-CD19 antibodies and propidium iodide. The cell cycle distribution of the CD19(+) and hence successfully transfected cells was determined by FACS analysis. The results shown here are the average of replicates and are representative of two independent experiments.

Immunoblots prepared from these extracts showed marked downregulation of the Cyclin D1 and D2 protein after adenoviral infection with either Ad-FKHR;AAA or Ad-FKHR;HRAAA. Loss of Cyclin D protein was accompanied by a loss of the phosphorylated forms of the protein product of the *RB-1* gene (pRB), the primary substrate of D-type cyclins (Figure 8A). Similar results were obtained in 786-O cells (Figure 4D and data not shown). In U87-MG cells, introduction of FKHR;AAA also induced an increase in p27, consistent with previously published data (Medema et al., 2000). FKHR;HRAAA, however, did not lead to a change in the levels of p27, yet retained the ability to downregulate D-type cyclins and to inhibit cell proliferation (Figure 8A). These data indicate that the induction of p27 is not necessary for the regulation of proliferation by FKHR.

In order to ask whether downregulation of D-type cyclins was required for the induction of a G1 arrest by FKHR, we next asked whether restoration of Cyclin D1 was sufficient to bypass a FKHR;AAA-induced cell cycle arrest. 786-O cells were transiently transfected with FKHR;AAA, along with plasmids encoding CD19 and either vector or Cyclin D1 and Cdk4. Expression of cyclin D1/cdk4 completely reversed the cell cycle arrest induced by FKHR;AAA (Figure 8B), while coexpression of a form of Cyclin D1 (Cyclin D1;KE) that fails to activate cdk4 was defective, making it unlikely that sequestration of p27 accounts for the override activity of Cyclin D1. Thus, FKHR can regulate cell cycle progression through the regulation of D-type cyclins.

## Discussion

Data from studies in *C. elegans* and in mammalian cells suggest that daf-16 and the daf-16-like transcription factors, FKHR, FKHRL1, and AFX, are central mediators of the transcriptional response to PI3K signaling. The functional outputs of these factors, including metabolic responses, apoptosis, cell cycle regulation, and stress responses, have been thought to depend primarily upon the interaction of these forkhead factors with an IRS promoter element and subsequent gene activation.

Here, we find that direct binding to an IRS is not required for the activation or repression of a number of FKHR transcriptional targets. Our data also suggest that this binding is not required for FKHR-dependent tumor suppression. Specifically, a mutant form of FKHR, which does not interact with an IRS element in vitro, does not bind to such promoter elements in vivo, and thus does not activate a class of genes that include prototypic IRS regulated genes such as *IGFBP-1*, nonetheless repressed transcription of a class of genes that includes D-type cyclins, bound to such promoters in vivo, and retained the cell cycle regulatory and tumor suppressor properties of FKHR.

Two possible mechanisms could account for IRS-independent gene regulation through FKHR and the presence of the FKHR;HRAAA mutant bound to Class II and III promoters. First, FKHR might interact with other transcription factors and modulate their activities. The Estrogen receptor (ERα), as an example, induces gene activation through both a classical estrogen receptor response (ERE) element and a nonclassical response element (AP-1) (Jakacka et al., 2001; Webb et al., 1999). In this model, it is also possible that at certain promoters, FKHR might bind simultaneously to an IRS element and to a second promoter site through an interaction with another transcription factor. Such a model might account for the retention of partial but not full activity of FKHR;HRAAA toward a number of the Class IIa transcripts. Whether such promoter and transcription factor interactions account, at least in part, for the regulation of Class II and III genes is under investigation.

Alternatively, the HR mutant of FKHR might retain direct DNA binding to a promoter element other than the classic IRS. The majority of the DNA contacts made by winged helix transcription factors such as HNF-3 and genesis are made through helix 3 lying in the DNA major groove. However, domains flanking helix 3 also make additional DNA contacts both with the phosphate backbone and with base atoms (Clark et al., 1993; Jin et al., 1999). Thus, it is possible that FKHR could interact with a new DNA response element present in Class IIa, IIb, and III without the requirement for the helix 3 Histidine residue.

Our data also suggest that transcriptional inhibition of D-type cyclins, rather than gene activation (of Class I genes for example), accounts for tumor suppression linked to FKHR. A concern here is that expression of FKHR proteins might nonspecifically squelch transcription by competing away coactivators. Class III genes, however, comprised a small minority of the 54,684 cDNAs spotted on the complete genome array, the vast majority of which did not change in response to FKHR;HRAAA. Moreover, treatment of Ad-FKHR;AAA-infected cells with the histone deacetylase inhibitor trichostatin A reversed FKHR-mediated inhibition of Cyclin D1 and D2 (I.S. and W.R.S., unpublished data), strongly suggesting that FKHR can act as a specific transcriptional repressor for Class III genes. In functional experiments, FKHR;HRAAA retained the ability to suppress Cyclin D1 and D2 protein levels, induce a G1 arrest in 786-O cells, and suppress soft agar and xenograft growth. We have also tested FKHR mutants lacking the C-terminal transactivation domain and find that they likewise retain the ability to arrest cells in G1

and to suppress soft agar growth (I. S. and W.R.S., unpublished data). Thus, transactivation is not required. Taken together, these data suggest that tumor suppression by FKHR is linked to transcriptional repression rather than to gene activation. Our data also support the idea, put forth by a number of groups (Brunet et al., 1999; Dijkers et al., 2000; Tang et al., 1999), that forkhead factors require IRS binding activity in order to induce apoptosis. FKHR;HRAAA suppressed tumor xenograft formation in 786-O cells, but failed to induce apoptosis in LNCaP cells, raising the possibility that in such "apoptosis sensitive" cells, one might be able to test whether tumor suppression is or is not separable from IRS-dependent induction of apoptosis.

Medema et al. found that FKRHL1 and AFX could induce p27 protein and mRNA, and moreover that p27 null cells were partially resistant to an AFX-induced G1 arrest (Medema et al., 2000). In keeping with these data, we previously found that FKHR;AAA reintroduction results in a change in the protein half-life of p27 (Nakamura et al., 2000). These results suggested that forkhead growth suppression is due, at least in part, to the regulation of p27. Data presented here suggest that while p27 induction may yet be sufficient, it is not necessary for FKHR-mediated growth and tumor suppression. Similarly, this group has independently found that forkhead factors can transcriptionally downregulate D-type cyclins and this, at least in part, accounts for forkhead-mediated regulation of G1 progression (R. Medema, personal communication). In a genetic test of the relationship between PI3K-mediated proliferative signaling and p27 function, when *PTEN* heterozygous mice were mated with p27 heterozygous mice, a cooperative increase in the development of prostate cancers was noted (Di Cristofano et al., 2001). These in vivo data raised the possibility that PI3K-dependent proliferative signals are not simply redundant with p27 loss. Taken together, these data suggest that FKHR can regulate cell cycle progression through at least two mechanisms, induction of p27 and downregulation of D-type cyclins. This latter mechanism may begin to explain the in vivo synergy between p27 loss and deregulated PI3K signaling.

While the primary goal of these experiments was to understand the nature of FKHR's role as a cell cycle regulator and as a growth/tumor suppressor, it is of interest to note that several of the Class II genes appear to be involved in cellular responses to oxidative stress (*SOD2*, *GCLC*), osmotic stress (*SLC5A3*), and DNA damage (*DDB1* and Cyclin G2). In particular, *SOD2* plays key roles in responding to oxidative stresses. The mammalian SOD2 protein is a mitochondrial Mn-dependent superoxide dismutase encoded by the *SOD-2* gene located on chromosome 6. In *C. elegans,* there are 4 SOD genes. SOD2 and 3 are both Mn-dependent and SOD-3 is mitochondrial in localization. In *C. elegans*, mutations in *daf-2* or *age-1* that confer oxidative stress resistance (*oxr*) result in the induction of *sod-3* (Honda and Honda, 1999). A number of genes that are known to "respond" to DNA damage were also found in class II, including *DDB1* (Dualan et al., 1995), *BTG1* (Cortes et al., 2000), and Cyclin G2 (Bates et al., 1996). While this work was under review, a direct role for FKHRL1 induction of the *GADD45* gene in repairing DNA damage was demonstrated (Tran et al., 2002). In these same experiments, Cyclin G2 was also identified as a potential FKHRL1 transcriptional target.

As mentioned above, in *C. elegans,* mutations in *daf-2* and *age-1* lead to increased resistance to oxidative stress, UV, and heat (Honda and Honda, 1999). Our data, together with the emerging data in *C. elegans,* suggest that in mammalian cells, the daf-like FKHR family members play an important role in the cellular response to oxidative stress and a novel role in mediating the cellular response to DNA damage through the activation of class IIa and IIb genes.

Taken together, the data presented here support a novel mechanism underlying the activity of FKHR as a cell cycle regulator and tumor suppressor. Specifically, these activities are linked to FKHR recruitment to promoters through an IRS-independent mechanism and to downregulation of Class III targets, and are separable from IRS-dependent activation of classical IRS dependent promoters.

## Experimental procedures

### Cell lines, cell culture, retroviral infection, plasmid transfection, and MTS assay

LNCaP, 786-O, and U2-OS cells were maintained as previously described. U2-OS, $\phi$X-A cells were transfected by the BBS-$CaCl_2$ method, and retroviral supernatants produced as previously described (Pear et al., 1993; Sellers et al., 1998). 786-O cells were transfected using Fugene reagent (Roche Applied Science). LNCaP cell viability and U87-MG cell growth were assayed using the AQueous non-Radioactive Cell Proliferation Assay (Promega) as previously described (Nakamura et al., 2000). Cell cycle analysis and senescence-associated β-galactosidase staining were performed as previously described (Dimri et al., 1995; Sellers et al., 1998). Colony formation was determined by suspending 786-O cells in 2× DMEM with 0.3% agarose and plating on a layer of 0.6% agarose in DMEM. Cells were fed every 3 days with 2× DMEM containing 0.3% agarose. Xenograft growth was determined by injecting $1 \times 10^5$ cells from the second passage of retrovirally transduced 786-O cells into the flanks of $nu^{-/-}$ female mice (Taconic) in 100 μl PBS. Detectable tumors were measured weekly and mice were sacrificed when any tumor measurement exceeded 1.5 cm.

### Plasmids

The plasmids pCDNA3-Flag-FKHR, pCDNA3-Flag-FKHR;H215R, pCDNA3-Flag-FKHR;AAA, pBABE-puroL, pBABE-puroL-HA-FKHR, pBABE-puroL-HA-FKHR;AAA, pBABE-puroL-HA-FKHR;H215R, pCMV-βGal, pCD19, and pGL2promoter-3xIRS were described previously (Nakamura et al., 2000). pRcCMV-Cyclin D1;WT, pRcCMV-Cyclin D1;KE, and pRcCMV-CDK4 were the gift of J. Lamb and M. Ewen and were described previously (Neuman et al., 1997); pCDNA3-Flag-FKHR;HRAAA was the gift of E. Tang, F. Barr, and K. Guan (Tang et al., 1999). pAD-Track-CMV was the gift of K. Polyak and B. Vogelstein. Inserts liberated by partial HindIII and complete XbaI digestion of pCDNA3-Flag-FKHR;AAA and pCDNA3-Flag-FKHR;HRAAA were ligated to HindIII/XbaI-restricted pAD-TrackCMV to give pAD-Track-Flag-FKHR;AAA and pAD-Track- Flag-FKHR;HRAAA. A PCR amplified insert of pCDNA3-Flag-FKHR;HRAAA was digested with BamH1/XhoI and ligated to similarly restricted pBABE-puroL-HA to give pBABE-puroL-HA-FKHR;HRAAA.

### Generation of adenoviruses

Ad.FKHR;AAA and Ad.FKHR;HRAAA were generated with the pAD-Easy system (He et al., 1998). Briefly, linearized shuttle plasmids were cotransfected with pAdEasy-1 into BJ5183 cells. After isolation, recombinant adenoviral DNA was restricted with PacI and transfected into 293 cells. Infectious adenovirus was amplified in 293 cells. Purified virus was isolated by freeze-thaw extraction followed by CsCl gradient purification and titered by plaque lysis.

### Antibodies, immunoblotting, protein extraction, and luciferase assays

M5 anti-Flag antibody (Sigma) was used at 10 μg/ml. HA.11 (Covance), anti-GSK3, anti-phospho-GSK3, anti-phospho-Akt, anti-Akt (all from Cell Signaling Technology), anti-p27 antibody (Transduction laboratories), G3-245 anti-RB antibody (Pharmingen), anti-Cyclin D1 antibody (NeoMaker), anti-Cdk4 antibody (C-22, Santa Cruz), and Cyclin D2 antibody (M-20 Santa Cruz) were used at a dilution of 1:1000. Anti-GAPDH (Biodesign International)

was used at 1:5000. Anti IGFBP1 (Biogenesis) and anti-Cbl-B antibody (H121, Santa Cruz) were used at a dilution of 1:500. Anti MxiI antibody (BD BioScience) was used at a dilution of 1:250. Luciferase and β-galactosidase activity assays were performed as previously described (Sellers et al., 1998).

**Electrophoretic mobility shift assay**

Cells were lysed in 50 mM Tris (pH 8.0), 100 mM NaCl, 2 mM EGTA, 10 mM NaF, 40 mM β-gycerolphosphate, 0.5% Triton-X100, 2 mM DTT, 1 mM aprotinin, and 1 mM PMSF. $^{32}$P labeled annealed double-stranded oligonucleotides containing the IGFBP-1 IRS site (5′-CACTAGCAAAACAAACTTAT TTTGAACAC-3′) were prepared as previously described (Tang et al., 1999). Binding reactions were carried out for 20 min at RT in 20 mM HEPES (pH 7.9), 150 mM KCl, 2 mM $MgCl_2$, 0.1 mg/ml BSA, 5 mM DTT, 1 mM PMSF, and 10 μg of sonicated salmon testis DNA with 1 μg protein extract and 1 ng of labeled probe. Where indicated, the extract was preincubated with 1 μl of anti-Flag antibody for 5 min. Protein-DNA complexes were resolved by native gel electrophoresis and visualized by autoradiography.

**cDNA microarray construction, array hybridization, data analysis, and real-time PCR**

Nylon filters were spotted with individual cDNA clones as previously described (Chiang et al., 2001). A detailed description of these methods used to generate and probe the arrays can be found in the Supplemental Experimental Procedures at http://www.cancercell.org/cgi/content/full/2/1/81/DC1. Experiments 1 and 2 used a 30,000 clone array (30 K), while experiment 3 was analyzed on a "complete genome" (CG) array.

Total RNA, isolated using the Qiagen RNeasy kit, was reverse transcribed and labeled as previously described (Chiang et al., 2001). Radiolabeled cDNA was hybridized at $2 \times 10^6$ cpm/ml to array filters at 65°C overnight. Filters were exposed to phosphoimager screens for 60 hr. Hybridization signals were captured by phosphoimaging (Fuji) and digitized to give an intensity value using ARRAY VISION software (Imaging Research). All array hybridizations were performed in duplicate. Array intensities were normalized to the median of the arrays for each experiment. The minimum intensity threshold for each experiment was found by comparing the intensities of replicates on scatter plots and determining the average coefficient of variation at any given intensity. Scatter plots of replicate arrays, performed after normalization, showed highly reproducible data (average coefficient of variation less than 0.4) above an absolute expression intensity of 0.8.

Clones whose expression did not change more than 1.5 fold (for example, 31,763 clones for CG array) or whose absolute hybridization intensity did not reach a value of 0.8 in at least one sample were filtered (9,033 clones on the CG array), leaving 16,548 clones out of 56,844 clones for further analysis. Data were then analyzed using GeneSpring software (Silicon Genetics) to select genes regulated by FKHR. The data were normalized to the Ad-vector time 0 data point, and the average of replicate hybridizations was plotted as fold change with time after infection. Absolute hybridization intensities were also plotted with time after treatment. These data were then analyzed by K-means clustering or by hierarchical clustering as described in the results.

The detailed methods for Real-Time PCR analysis, including the primer set used, can be found in the Supplemental Experimental Procedures.

**Chromatin immunoprecipitation (ChIP)**

ChIP experiments were performed as described previously (Shang et al., 2000). Briefly, 786-O cells infected with the adenoviral vector or adenovirus expressing either FKHR;AAA or FKHR;HRAAA were washed twice with PBS at RT and fixed in 1% formaldehyde in PBS at 4°C for 20 min. Fixed cells were washed twice with PBS at 4°C and lysed for 10 min in 300 μl of 1%SDS, 5 mM EDTA, and 50 mM Tris-HCl (pH 8.1) at 4°C. Chromatin was sheared by sonicating three times for 15 s at a setting of 30 (Fisher Sonic Dismembrator, Model 300) followed by centrifugation for 10 min at 14000 rpm. Twenty μl of the resulting supernatant was set aside as input chromatin and the remainder diluted 1:10 in 1% Triton X-100, 2 mM EDTA, 150 mM NaCl, and 20 mM Tris-HCl (pH 8.1). Diluted supernatants were precleared for 2 hr at 4°C with 2 μg sonicated salmon sperm DNA (sssDNA) and 45 μl of 50% (v/v) protein G sepharose in 10 mM Tris-HCl (pH 8.1), 1 mM EDTA per ml. Supernatants were collected and incubated with 10 μl of anti FLAG antibody (M5) overnight, followed by the addition of 2 μg sssDNA and 45 μl of 50% v/v protein G beads. Protein G bound complexes were serially washed with TSEI (0.1%SDS, 1% Triton X-100, 2 mM EDTA, 20 mM Tris-HCl (pH 8.1), and 150 mM NaCl), TSEII (0.1%SDS, Triton X-100, 2 mM EDTA, 20 mM Tris-HCl [pH 8.1], and 500 mM NaCl), buffer III (0.25 M LiCl, 1% NP-40, 1% deoxycholate, 1 mM EDTA, and 10 mM Tris-HCl [pH 8.1]), and finally with TE. Bound DNA was eluted by incubating the beads in 100 μl of 1% SDS and 0.1 M $NaHCO_3$) for 8 hr at 65°C. The input DNA was diluted with 80 μl of PBS and incubated at 65°C for 8 hr. DNA was purified using the PCR purification kit (Qiagen). The indicated promoter fragments were detected with the primers as indicated in Figure 5.

**Acknowledgments**

The authors would like to acknowledge the significant contribution of the transcription profiling core group at Millennium Pharmaceuticals who prepared the arrays and conducted the hybridization of cDNA probes, and without whom this work would not have been possible. S.R. was supported by a grant from the Mass Department of Public Health (41211159028), and W.R.S. was supported by grants from the National Cancer Institute (CA85912), the Department of Defense (DAMD17-98-1-8596), and the Damon Runyon Cancer Research Foundation.

Received: June 7, 2002
Revised: June 26, 2002

**References**

Ayala, J.E., Streeper, R.S., Desgrosellier, J.S., Durham, S.K., Suwanichkul, A., Svitek, C.A., Goldman, J.K., Barr, F.G., Powell, D.R., and O'Brien, R.M. (1999). Conservation of an insulin response unit between mouse and human glucose-6-phosphatase catalytic subunit gene promoters: transcription factor FKHR binds the insulin response sequence. Diabetes *48*, 1885–1889.

Bates, S., Rowan, S., and Vousden, K.H. (1996). Characterisation of human cyclin G1 and G2: DNA damage inducible genes. Oncogene *13*, 1103–1109.

Biggs, W.H., 3rd, Meisenhelder, J., Hunter, T., Cavenee, W.K., and Arden, K.C. (1999). Protein kinase B/Akt-mediated phosphorylation promotes nuclear exclusion of the winged helix transcription factor FKHR1. Proc. Natl. Acad. Sci. USA *96*, 7421–7426.

Brunet, A., Bonni, A., Zigmond, M.J., Lin, M.Z., Juo, P., Hu, L.S., Anderson, M.J., Arden, K.C., Blenis, J., and Greenberg, M.E. (1999). Akt promotes cell survival by phosphorylating and inhibiting a Forkhead transcription factor. Cell *96*, 857–868.

Cheney, I.W., Johnson, D.E., Vaillancourt, M.T., Avanzini, J., Morimoto, A., Demers, G.W., Wills, K.N., Shabram, P.W., Bolen, J.B., Tavtigian, S.V., and Bookstein, R. (1998). Suppression of tumorigenicity of glioblastoma cells by adenovirus-mediated MMAC1/PTEN gene transfer. Cancer Res. *58*, 2331–2334.

Chiang, L.W., Grenier, J.M., Ettwiller, L., Jenkins, L.P., Ficenec, D., Martin, J., Jin, F., DiStefano, P.S., and Wood, A. (2001). An orchestrated gene expression component of neuronal programmed cell death revealed by cDNA array analysis. Proc. Natl. Acad. Sci. USA *98*, 2814–2819.

Clark, K.L., Halay, E.D., Lai, E., and Burley, S.K. (1993). Co-crystal structure of the HNF-3/fork head DNA-recognition motif resembles histone H5. Nature *364*, 412–420.

Cortes, U., Moyret-Lalle, C., Falette, N., Duriez, C., Ghissassi, F.E., Barnas, C., Morel, A.P., Hainaut, P., Magaud, J.P., and Puisieux, A. (2000). BTG gene expression in the p53-dependent and-independent cellular response to DNA damage. Mol. Carcinog. *27*, 57–64.

del Peso, L., Gonzalez, V.M., Hernandez, R., Barr, F.G., and Nunez, G. (1999). Regulation of the forkhead transcription factor FKHR, but not the PAX3-FKHR fusion protein, by the serine/threonine kinase Akt. Oncogene *18*, 7328–7333.

Di Cristofano, A., De Acetis, M., Koff, A., Cordon-Cardo, C., and Pandolfi, P.P. (2001). Pten and p27KIP1 cooperate in prostate cancer tumor suppression in the mouse. Nat. Genet. *27*, 222–224.

Dijkers, P.F., Medema, R.H., Lammers, J.W., Koenderman, L., and Coffer, P.J. (2000). Expression of the pro-apoptotic Bcl-2 family member Bim is regulated by the forkhead transcription factor FKHR-L1. Curr. Biol. *10*, 1201–1204.

Dimri, G.P., Lee, X., Basile, G., Acosta, M., Scott, G., Roskelley, C., Medrano, E.E., Linskens, M., Rubelj, I., Pereira-Smith, O., et al. (1995). A biomarker that identifies senescent human cells in culture and in aging skin in vivo. Proc. Natl. Acad. Sci. USA *92*, 9363–9367.

Dualan, R., Brody, T., Keeney, S., Nichols, A.F., Admon, A., and Linn, S. (1995). Chromosomal localization and cDNA cloning of the genes (DDB1 and DDB2) for the p127 and p48 subunits of a human damage-specific DNA binding protein. Genomics *29*, 62–69.

Eisen, M.B., Spellman, P.T., Brown, P.O., and Botstein, D. (1998). Cluster analysis and display of genome-wide expression patterns. Proc. Natl. Acad. Sci. USA *95*, 14863–14868.

Furnari, F.B., Lin, H., Huang, H.S., and Cavenee, W.K. (1997). Growth suppression of glioma cells by PTEN requires a functional phosphatase catalytic domain. Proc. Natl. Acad. Sci. USA *94*, 12479–12484.

Furnari, F.B., Huang, H.J., and Cavenee, W.K. (1998). The phosphoinositol phosphatase activity of PTEN mediates a serum-sensitive G1 growth arrest in glioma cells. Cancer Res. *58*, 5002–5008.

Hall, R.K., Yamasaki, T., Kucera, T., Waltner-Law, M., O'Brien, R., and Granner, D.K. (2000). Regulation of phosphoenolpyruvate carboxykinase and insulin-like growth factor-binding protein-1 gene expression by insulin. The role of winged helix/forkhead proteins. J. Biol. Chem. *275*, 30169–30175.

He, T.C., Zhou, S., da Costa, L.T., Yu, J., Kinzler, K.W., and Vogelstein, B. (1998). A simplified system for generating recombinant adenoviruses. Proc. Natl. Acad. Sci. USA *95*, 2509–2514.

Herwig, R., Poustka, A.J., Muller, C., Bull, C., Lehrach, H., and O'Brien, J. (1999). Large-scale clustering of cDNA-fingerprinting data. Genome Res. *9*, 1093–1105.

Honda, Y., and Honda, S. (1999). The daf-2 gene network for longevity regulates oxidative stress resistance and Mn-superoxide dismutase gene expression in Caenorhabditis elegans. FASEB J. *13*, 1385–1393.

Jakacka, M., Ito, M., Weiss, J., Chien, P.Y., Gehm, B.D., and Jameson, J.L. (2001). Estrogen receptor binding to DNA is not required for its activity through the nonclassical AP1 pathway. J. Biol. Chem. *276*, 13615–13621.

Jin, C., Marsden, I., Chen, X., and Liao, X. (1999). Dynamic DNA contacts observed in the NMR structure of winged helix protein-DNA complex. J. Mol. Biol. *289*, 683–690.

Kops, G.J., de Ruiter, N.D., De Vries-Smits, A.M., Powell, D.R., Bos, J.L., and Burgering, B.M. (1999). Direct control of the Forkhead transcription factor AFX by protein kinase B. Nature *398*, 630–634.

Lin, K., Dorman, J.B., Rodan, A., and Kenyon, C. (1997). daf-16: An HNF-3/forkhead family member that can function to double the life-span of Caenorhabditis elegans. Science *278*, 1319–1322.

Maehama, T., and Dixon, J.E. (1999). PTEN: a tumour suppressor that functions as a phospholipid phosphatase. Trends Cell Biol. *9*, 125–128.

Medema, R.H., Kops, G.J., Bos, J.L., and Burgering, B.M. (2000). AFX-like Forkhead transcription factors mediate cell-cycle regulation by Ras and PKB through p27kip1. Nature *404*, 782–787.

Nakamura, N., Ramaswamy, S., Vazquez, F., Signoretti, S., Loda, M., and Sellers, W.R. (2000). Forkhead transcription factors are critical effectors of cell death and cell cycle arrest downstream of PTEN. Mol. Cell. Biol. *20*, 8969–8982.

Neuman, E., Ladha, M.H., Lin, N., Upton, T.M., Miller, S.J., DiRenzo, J., Pestell, R.G., Hinds, P.W., Dowdy, S.F., Brown, M., and Ewen, M.E. (1997). Cyclin D1 stimulation of estrogen receptor transcriptional activity independent of cdk4. Mol. Cell. Biol. *17*, 5338–5347.

Ogg, S., Paradis, S., Gottlieb, S., Patterson, G.I., Lee, L., Tissenbaum, H.A., and Ruvkun, G. (1997). The Fork head transcription factor DAF-16 transduces insulin-like metabolic and longevity signals in C. elegans. Nature *389*, 994–999.

Pear, W.S., Nolan, G.P., Scott, M.L., and Baltimore, D. (1993). Production of high-titer helper-free retroviruses by transient transfection. Proc. Natl. Acad. Sci. USA *90*, 8392–8396.

Rena, G., Guo, S., Cichy, S.C., Unterman, T.G., and Cohen, P. (1999). Phosphorylation of the transcription factor forkhead family member FKHR by protein kinase B. J. Biol. Chem. *274*, 17179–17183.

Schmoll, D., Walker, K.S., Alessi, D.R., Grempler, R., Burchell, A., Guo, S., Walther, R., and Unterman, T.G. (2000). Regulation of glucose-6-phosphatase gene expression by protein kinase Balpha and the forkhead transcription factor FKHR. Evidence for insulin response unit-dependent and-independent effects of insulin on promoter activity. J. Biol. Chem. *275*, 36324–36333.

Schuur, E.R., Loktev, A.V., Sharma, M., Sun, Z., Roth, R.A., and Weigel, R.J. (2001). Ligand-dependent interaction of estrogen receptor-$\alpha$ with FKHR. J. Biol. Chem. *276*, 33554–33560.

Sellers, W.R., Novitch, B.G., Miyake, S., Heith, A., Otterson, G.A., Kaye, F.J., Lassar, A.B., and Kaelin, W.G., Jr. (1998). Stable binding to E2F is not required for the retinoblastoma protein to activate transcription, promote differentiation, and suppress tumor cell growth. Genes Dev. *12*, 95–106.

Shang, Y., Hu, X., DiRenzo, J., Lazar, M.A., and Brown, M. (2000). Cofactor dynamics and sufficiency in estrogen receptor-regulated transcription. Cell *103*, 843–852.

Takaishi, H., Konishi, H., Matsuzaki, H., Ono, Y., Shirai, Y., Saito, N., Kitamura, T., Ogawa, W., Kasuga, M., Kikkawa, U., and Nishizuka, Y. (1999). Regulation of nuclear translocation of forkhead transcription factor AFX by protein kinase B. Proc. Natl. Acad. Sci. USA *96*, 11836–11841.

Tang, E.D., Nunez, G., Barr, F.G., and Guan, K.L. (1999). Negative regulation of the forkhead transcription factor FKHR by Akt. J. Biol. Chem. *274*, 16741–16746.

Tomizawa, M., Kumar, A., Perrot, V., Nakae, J., Accili, D., Rechler, M.M., and Kumaro, A. (2000). Insulin inhibits the activation of transcription by a C-terminal fragment of the forkhead transcription factor FKHR. A mechanism for insulin inhibition of insulin-like growth factor-binding protein-1 transcription. J. Biol. Chem. *275*, 7289–7295.

Tran, H., Brunet, A., Grenier, J.M., Datta, S.R., Fornace, A.J., Jr., DiStefano, P.S., Chiang, L.W., and Greenberg, M.E. (2002). DNA repair pathway stimulated by the forkhead transcription factor FOXO3a through the Gadd45 protein. Science *296*, 530–534.

Vazquez, F., and Sellers, W.R. (2000). The PTEN tumor suppressor protein: an antagonist of phosphoinositide 3-kinase signaling. Biochim. Biophys. Acta *1470*, M21–M35.

Webb, P., Nguyen, P., Valentine, C., Lopez, G.N., Kwok, G.R., McInerney, E., Katzenellenbogen, B.S., Enmark, E., Gustafsson, J.A., Nilsson, S., and Kushner, P.J. (1999). The estrogen receptor enhances AP-1 activity by two distinct mechanisms with different requirements for receptor transactivation functions. Mol. Endocrinol. *13*, 1672–1685.

Weigelt, J., Climent, I., Dahlman-Wright, K., and Wikstrom, M. (2001). Solution structure of the DNA binding domain of the human forkhead transcription factor AFX (FOXO4). Biochemistry *40*, 5861–5869.

Yeagley, D., Guo, S., Unterman, T., and Quinn, P.G. (2001). Gene- and activation- specific mechanisms for insulin inhibition of basal and glucocorticoid-induced IGFBP-1 and PEPCK transcription: Roles of forkhead and insulin response sequences. J. Biol. Chem. *276*, 33705–33710.

Zhao, H.H., Herrera, R.E., Coronado-Heinsohn, E., Yang, M.C., Ludes-Meyers, J.H., Seybold-Tilson, K.J., Nawaz, Z., Yee, D., Barr, F.G., Diab, S.G., et al. (2001). Forkhead homologue in rhabdomyosarcoma functions as a bifunctional nuclear receptor-interacting protein with both coactivator and corepressor functions. J. Biol. Chem. *276*, 27907–27912.